Vibrationally and rotationally nonadiabatic calculations on H_3^+ using coordinate-dependent vibrational and rotational masses

Leonardo G. Diniz[*]

Laboratório de Átomos e Moléculas Especiais, Departamento de Física, ICEx, Universidade Federal de Minas Gerais, Av. Antônio Carlos 6627, 31270-901 Belo Horizonte - MG, Brazil and Centro Federal de Educação Tecnológica de Minas Gerais, Unidade VII, Brazil

José Rachid Mohallem[†]

Laboratório de Átomos e Moléculas Especiais, Departamento de Física, ICEx, Universidade Federal de Minas Gerais, Av. Antônio Carlos 6627, 31270-901 Belo Horizonte - MG, Brazil

Alexander Alijah[‡]

Groupe de Spectrométrie Moléculaire et Atmosphérique, GSMA, UMR CNRS 7331, Université de Reims Champagne-Ardenne, U.F.R. Sciences Exactes et Naturelles, Moulin de la Housse Boîte Postale 1039, 51687 Reims Cedex 2, France

Michele Pavanello[§]

Department of Chemistry, Rutgers University, Newark, New Jersey 07003, USA

Ludwik Adamowicz[‖]

Department of Chemistry and Biochemistry, the University of Arizona, Tucson, Arizona 85721, USA

Oleg L. Polyansky[¶] and Jonathan Tennyson[**]

Department of Physics and Astronomy, University College London, Gower Street, London WC1E 6BT, United Kingdom

Using the core-mass approach, we have generated a vibrational-mass surface for the triatomic H_3^+. The coordinate-dependent masses account for the off-resonance nonadiabatic coupling and permit a very accurate determination of the rovibrational states using a single potential energy surface. The new, high-precision measurements of 12 rovibrational transitions in the ν_2 bending fundamental of H_3^+ by Wu *et al.* [Phys. Rev. A **88**, 032507 (2013)] are used to scale this surface empirically and to derive state-dependent vibrational and rotational masses that reproduce the experimental transition energies to 10^{-3} cm^{-1}. Rotational term values for $J \leqslant 10$ are presented for the two lowest vibrational states and equivalent transitions in D_3^+ considered.

PACS number(s): 31.10.+z, 31.15.B−, 33.20.Ea

I. INTRODUCTION

The smallest polyatomic ion H_3^+ has been the subject of several, recent theoretical and experimental investigations. Despite having only two electrons, accurate modeling of H_3^+ spectroscopy is far from being a trivial task. Prompted by the need of the astronomy community to characterize the spectrum of H_3^+ [1], recent works [2–8] have focused on its high-lying rovibrational energy states. Especially elusive [9] had been the states lying above the so-called barrier to linearity, i.e., 10 000 cm^{-1} above the zero-point level or 14 360 cm^{-1} above the bottom of the potential energy surface (PES). These states can access linear H_3^+ configurations with non-negligible probability. Theoretical shortcomings had not allowed for a meaningful comparison with the experiment

in this high-energy region until the very recent works of Alijah [2], Pavanello *et al.* [3,4,6], and Jaquet *et al.* [7,8].

Until now the rovibrational spectrum of H_3^+ has been measured with 0.01 cm^{-1} accuracy [10]. In a new experiment, Wu *et al.* [11] measured 12 rovibrational transitions between the vibrational ground state $(v_1, v_2^{|\ell|}) = (0, 0^0)$ and the first vibrational excited state $(0, 1^1)$ of H_3^+ with unprecedented accuracy of about 10^{-4} cm^{-1}. These new measurements constitute a unique test bed for high-accuracy calculations.

On the theoretical side, Pavanello *et al.* [3,4] recently presented a very accurate global H_3^+ PES, called GLH3P, which included diagonal adiabatic and relativistic corrections. Pavanello and co-workers used this PES to calculate rovibrational states located up to 5000 cm^{-1} above the barrier to linearity. This PES is also employed here as the potential in the nuclear Schrödinger equation, from which the rovibrational levels are determined. The ambiguity which still remains in the nuclear Schrödinger equation is what masses one should use to best describe the nuclear rovibrational motion [12]. The choice of these masses is the main topic of the present study.

In very accurate rovibrational calculations one needs to account for the fact that when nuclei displace during the vibrational motion some of the electron density, particularly that associated with the core electrons, follows the motion

―――――――
[*]leofisica@yahoo.com.br
[†]rachid@fisica.ufmg.br
[‡]alexander.alijah@univ-reims.fr
[§]m.pavanello@rutgers.edu
[‖]ludwik@u.arizona.edu
[¶]o.polyansky@ucl.ac.uk
[**]j.tennyson@ucl.ac.uk

of the nuclei. This increases somewhat the masses of the moving nuclei. This effect is called the nonadiabatic coupling and it is usually accounted for using the perturbation theory where the first order correction to the electronic wave function is expanded in terms of higher electronic states. Far from curve crossings one can also use an effective treatment in accounting for this effect which involves modifying the nuclear masses used in the rovibrational calculations. This has been suggested by Bunker and Moss [13,14]; their theory leads to coordinate-dependent effective masses. Moss [15] derived optimized constant masses for the H_2^+ system based on fully nonadiabatic calculations; these have become known as Moss masses. Jaquet and Kutzelnigg [16], in their study of H_2^+ and D_2^+, concluded that for isolated electronic states nonadiabatic effects on rovibrational states "have mainly to do with the participation of the electrons in the nuclear motion and hardly with a coupling of different electronic states," which supports the development of an effective-mass approach considered in this work. In the above-mentioned H_3^+ rovibrational calculations by Pavanello *et al.* an effective-mass approach based on the Polyansky-Tennyson (PT) model [17] was employed. In this model the Moss H_2^+ mass [15] is used as the effective vibrational H_3^+ mass, while the rotational mass is kept as the bare-nuclear mass. The accuracy achieved for H_3^+ by using the PT model was better than 0.2 cm^{-1}. The recent high J calculations of Jaquet and Carrington [8] are also based on the PT model. A fixed effective mass determined directly for H_3^+, which would lead to improvement of these results, has not, to our knowledge, been reported yet.

Mohallem and co-workers [18,19] recently proposed an alternative procedure based on a separation of motions of core and valence electrons which uses core masses as the vibrational masses and empirical masses for the rotational masses. They tested those masses in calculations for H_2, H_2^+, and deuterated isotopologues. As the masses are coordinate dependent, better results were obtained than those computed with the constant Moss masses. In the present work, the Mohallem *et al.* model is applied to H_3^+ and a vibrational-mass surface is generated. The theoretical results for rovibrational states calculated with this surface are better than the PT results by about one order of magnitude. The results of the effective-mass calculations can further be improved by simple empirical scaling of the masses developed based on experimental data. Such data are now provided by Wu *et al.* Their results (with $J \leqslant 4$) are used in this work to determine effective empirical vibrational and rotational masses. These masses give the best possible agreement with the experimental data within the effective-mass model. The empirical masses are also used in this work to predict rovibrational term values for higher J states ($J \leqslant 10$) of the two lowest vibrational states.

II. THEORY

In highly accurate calculations of molecular rovibrational states the Born-Oppenheimer and adiabatic approximations might be too crude even for an off-resonance situation where the electronic state of interest is well separated from higher electronic states. This is, in particular, true for light molecules, as the neglected nonadiabatic terms scale as one over the reduced mass. For H_3^+ in the electronic ground state the effect

of the coupling to higher electronic states on the calculated rovibrational energies amounts to at least about 1 cm^{-1} in the energy region of up to 15 000 cm^{-1}. In general, when the nonadiabatic coupling between electronic states becomes strong, a system of coupled nuclear-motion equations needs to be solved to obtain accurate rovibrational energies. When the coupling is weak, which happens in the off-resonance case, a similarity transformation of the Hamiltonian can be performed that moves much of the nonadiabatic coupling to the diagonal (i.e., the PES) and the need to deal with the system of coupled equations can be avoided. Such an approach was developed by Bunker and Moss [13,14]. It preserves the useful concept of a single PES. As Bunker and Moss showed, it is mathematically possible to represent such a transformation by making the reduced masses become functions of the internuclear distances. Furthermore, they suggested using different vibrational reduced masses from the rotational reduced masses. In their original work on H_2 and H_2^+ [15,20,21], Bunker and Moss replaced these coordinate-dependent masses by constant effective masses. These masses have become known as Moss masses. Other authors applied the idea of effective constant masses also to H_3^+. In one such approach the constant mass used for each nucleus in H_3^+ was the proton mass augmented with two-thirds of the electron mass [22,23]. This mass was denoted as $NU23$ [24]. However better results were obtained when the Moss mass derived for H_2^+ was used instead [17]. This mass was roughly the proton mass augmented with about half the mass of an electron (see below). For a discussion of the different choices of masses see [25].

It should be noted that, due to the weak coupling of the nuclear rotations with the electronic degrees of freedom, the rotational nonadiabatic effect is much smaller than the vibrational nonadiabatic effect. Thus, for the rotational reduced mass, the nuclear reduced mass can be used in the first approximation. In our recent investigation of highly excited rovibrational states of H_3^+ situated above the barrier to linearity, we applied the PT model (the Moss vibrational mass and the nuclear rotational mass) and obtained the most accurate *ab initio* predictions of the rovibrational levels to date [3,4]. The Bunker and Moss nonadiabatic model was also used by Schwenke for H_2^+ and HD$^+$ [26], and for H_2 and water [27]. Though all terms in his work were calculated *ab initio*, in the end some scaling of the results was found necessary to bring the results in better agreement with the experiment. One should also mention the work of Jaquet and Khoma [28,29] where they made use of the Herman and Asgharian [30] approach to generate coordinate-dependent nuclear masses in investigating rovibrational spectra of H_2^+ and H_2. They also discussed the feasibility of applying the approach to H_3^+ and showed two plots of a yet incomplete vibrational-mass surface restricted to configurations with the C_{2v} symmetry. In the present work, we employ the methodology suggested by Mohallem *et al.* [18] to obtain effective masses for H_3^+. A complete mass surface is generated and presented in a functional form.

A. Vibrational-mass surface

In the recent paper [19], three of the present authors tested the effective-mass approach proposed by Mohallem *et al.* [18]. The tests involved constructing vibrational masses

from the so-called atomic core masses. These core masses were obtained from the Mulliken population analysis [31] of the electronic charge distribution at the nuclei forming the system. The atomic electronic charges obtained from the Mulliken analysis have two types of components, diagonal and off-diagonal. Each diagonal component depends on the atomic orbitals belonging to the same atom, while each off-diagonal component depends on atomic orbitals of two different atoms. These latter components, as associated with the electronic charge densities on the bonds, are not included in the atomic electronic charges used here. By adding the mass m_I of the nucleus I to the mass of the electrons at this nucleus, equal to the negative of the Mulliken electronic charge n_I at nucleus I, the effective vibrational mass of the I nucleus is obtained:

$$m_I(\vec{R}) = m_I + n_I(\vec{R})m_e. \tag{1}$$

Such an approach is based on an assumption that, when the I nucleus vibrates, this fraction of the total number of electrons vibrates with it. The vibrational reduced mass is then derived from the effective masses of the nuclei calculated according to (1). As the effective masses are coordinate dependent, a mass surface for the considered molecular system can be generated. Our test calculations performed for H_2 and H_2^+, and their deuterated isotopologues, showed that the effective coordinate-dependent masses determined this way lead to significantly more accurate results for the rovibrational frequencies than the results obtained with constant masses [19]. In the present work we test the variable-mass approach in the calculations of rovibrational states of the H_3^+ molecule. A vibrational-mass surface is generated and used in the rovibrational calculations.

In general, the effective vibrational masses of the three nuclei in the H_3^+ molecule do not need to be the same. Unequal masses would be required, for example, to describe the highly excited vibrational states near the lowest dissociation threshold corresponding to fragmentation of the system into H_2 and H^+, where interesting behavior is to be expected [32]. However, for the low-energy vibrational excitations considered in this work, it is reasonable to assume equal masses for the three nuclei. Thus, the three masses $m_A(\vec{R})$, $m_B(\vec{R})$, and $m_C(\vec{R})$ are symmetrized by adding to each nuclear mass m_I, $I = A, B, C$, a mass equal to the average number of electrons per nucleus, $\bar{n}(\vec{R})$:

$$\bar{m}_I(\vec{R}) = m_I + \frac{n_{AA}(\vec{R}) + n_{BB}(\vec{R}) + n_{CC}(\vec{R})}{3} m_e$$
$$= m_I + \bar{n}(\vec{R}) m_e. \tag{2}$$

$\bar{n}(\vec{R})$ is expressed, in the spirit of a many-body expansion of the potential energy surface [33], as a sum of one-body, two-body, and three-body terms,

$$\bar{n}(\vec{R}) = n^{(1)} + \sum_{i=1}^{3} n^{(2)}(R_i) + \bar{n}^{(3)}(\vec{R}). \tag{3}$$

The constant one-body term $n^{(1)}$ is the average number of electrons that remains at each of the three nuclei upon their complete separation. The two-body terms $n^{(2)}(R)$ account for the modification of the one-body term in the situation when any two nuclei are close to each other and strongly interact

while the third one is further away. The three-body term $\bar{n}^{(3)}(\vec{R})$ accounts for modification of the one- and two-body terms when all three nuclei strongly interact. Both, the two-body terms and the three-body term, vanish at the complete dissociation (atomization) of the system.

The possible three dissociation channels of H_3^+, where the molecule separates into a two-atom fragment and a one-atom fragment, identify the diatomic fragments. As the lowest dissociation limit for H_3^+ is $H_2(X\,^1\Sigma_g^+) + H^+$, all three two-body terms are equal and can be expressed as

$$n^{(2)}(R_i) = \frac{2}{3}\left[n_{H_2}(R_i) - 1\right], \quad i = 1, 2, 3, \tag{4}$$

where $n_{H_2}(R)$ is the fractional number of electrons at each hydrogen in H_2 in the ground state ($\tilde{X}\,^1\Sigma_g^+$). In the limit of $R \to \infty$, the charge on each nucleus of H_2 must be that of an isolated hydrogen atom, which means $\lim_{R \to \infty} n_{H_2}(R) = 1$. To make the two-body term vanish at large R, this limit has to be subtracted from $n_{H_2}(R)$. The factor of 2/3 accounts for the fact that H_3^+ is an ion and has only two electrons. In the limit of the complete dissociation $H_3^+ \to 2H + H^+$ the average charge density is given by the one-body term which is

$$n^{(1)} = \frac{2}{3}. \tag{5}$$

In this limit, the effective atomic mass becomes

$$m_I(\infty, \infty, \infty) = m_I + \frac{2}{3}m_e. \tag{6}$$

This is the so-called *NU23* mass [24,34].

Two comments need to be made here. First, due to symmetrization of the three masses, the separation into $2H + H^+$ cannot be described by the model. This, however, does not pose a problem in the calculation when only low-energy bound vibrational states are considered. Second, the united atom limits corresponding to one, two, or all three internuclear distances approaching zero are not strictly implemented. This could have been done analogously to the double many-body expansion (DMBE) for the potential energy surface [35], but was not considered relevant, as these configurations have very high energies and are not accessed by bound-state vibrations.

As mentioned, the effective electronic charges on the nuclei are determined in this work through the Mulliken population analysis. The analysis is performed using the GAMESS package [36,37]. In our previous work we computed the Mulliken charges for H_2 on a dense grid $0.2a_0 \leqslant R_i \leqslant 12a_0$, $\Delta R_i = 0.05a_0$, at the CI/cc-pV5Z level of theory. These data were interpolated using cubic splines. The same level of theory is applied in this work to calculate the Mulliken charges for H_3^+. The calculations are done for 187 geometrical configurations of the system, which comprise the "classic" 69 MBB (Meyer, Botschwina, Burton) [38] configurations augmented with the additional 118 configurations suggested by Polyansky *et al.* [39]. Next, the Mulliken charges are fitted with a polynomial expressed in terms of transformed symmetry coordinates, Q_i (see, for example, Refs. [4,40]), as

$$n^{(3)}(\vec{R}) = \sum_{i,j,k} c_{ijk}\, Q_1^i Q_2^j Q_3^k\, T(Q_1), \quad i + 2j + 3k \leqslant N. \tag{7}$$

The Q_i coordinates define the integrity basis [41],

$$Q_1 = S_a, \quad Q_2 = S_x^2 + S_y^2, \quad Q_3 = S_x(S_x^2 - 3S_y^2), \tag{8}$$
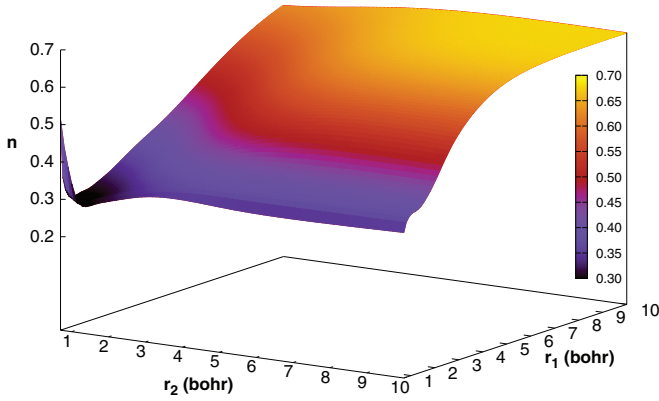
FIG. 1. (Color online) Visualization of the vibrational mass surface for configurations with the C_{2v} symmetry. r_1 is the atom-diatom distance and r_2 is the diatomic distance.

in terms of S_a, S_x, and S_y, which are the usual symmetry coordinates. Following Meyer *et al.* [38], the symmetry coordinates are represented as Morse coordinates $\tilde{R}_i$,

$$\tilde{R}_i = [1 - e^{-\beta(R_i/R_0 - 1)}]/\beta, \quad (9)$$

where R_i are the internuclear distances and $\beta = 1.3$ and $R_0 = 1.65 a_0$ are the expansion parameters. T is the following range-determining factor ensuring that the three-body term goes to zero at large distances:

$$T(x) = [1 + e^{\gamma(x - x_0)}]^{-1}, \quad (10)$$

with $\gamma = 0.2 a_0^{-1}$ and $x_0 = 11.0 a_0$. A ten-degree polynomial with 67 adjustable parameters is used in the fitting. Configurations with one or more internuclear distances smaller than $0.7 a_0$ are omitted from the fit. As their energies are very high, they are not relevant in the calculations of bound states. The root mean square error E_{RMS} of the fit is RMS $= 6.16 \times 10^{-4}$. Figure 1 shows this surface for symmetrical configurations using the Jacobi coordinates. Near the equilibrium configuration $r_1 = 1.65 a_0$ and $r_2 = 1.845 a_0$, the electronic contribution to the vibrational mass amounts to about $0.3 m_e$. When both distances become large, it approaches the $NU23$ limit.

The present rovibrational calculations, which are based on our latest, very accurate potential energy surface, GLH3P, incorporating diagonal adiabatic and relativistic corrections [3,4], are performed with two codes: the DVR3D code [42] for the initial vibrational calculations, owing to its efficiency, and the hyperspherical code [43] for the final rovibrational calculations, as it permits use of full symmetry. As neither of these codes allows for directly using coordinate-dependent masses in the kinetic energy operator, the following iterative procedure, used before in our calculations on H_2 and H_2^+ and deuterated isotopologues [19], is employed:

$$\overline{m}_{I,v_1,v_2,l}^{(i+1)} = m_I + m_e \int \overline{n}(\vec{R}) \big[\chi_{v_1,v_2,l}^{(i)}(\vec{R}) \big]^2 d\vec{R}, \quad (11)$$

where $\chi_{v_1,v_2,l}^{(i)}(\vec{R})$ is the wave function calculated with the mass $\overline{m}_{v_1,v_2,l}^{(i)}$. Starting with the mass set to $\overline{m}_{I,v_1,v_2,l}^{(0)} = m_I$, the iteration process continues until self-consistency. It usually converges after one step.

Two tests have been performed to ascertain the accuracy of the procedure. Prior to the tests the Mulliken charges

have been calculated at all DVR points on a grid with 1100 configurations corresponding to 11 diatomic distances, ten values of the distance between the third particle and the center of mass of the first two, and ten values of the angular coordinate. The purpose of the first test was to verify if the new data are accurately reproduced by the fit. The test showed that the fit reproduces the data with RMS $= 5.4 \times 10^{-3}$. In the second test the vibrational states have been calculated on the Discrete Variable Representation (DVR) grid using the effective masses determined directly from the Mulliken analysis for each grid point. Though in this case the masses of the diatom are different from the third mass, the vibrational energies of the lowest states come out the same as obtained with the average mass defined in Eq. (2).

B. Rovibrational calculations using hyperspherical harmonics

Rovibrational calculations have been performed in the democratic hyperspherical coordinates defined by Johnson [44]. These hyperspherical coordinates are symmetric super-positions of the three systems of Jacobi coordinates. Thus, the symmetry with respect to the permutation of the three nuclei and with respect to inversion of the coordinate system is automatically implemented. A particularly effective hyper-spherical approach is that of the hyperspherical harmonics suggested by Wolniewicz [43]. The harmonics depend on five coordinates and describe the motion of a three-particle system on a given hypersphere. For H_3^+ this means that they describe the degenerate vibrational motion and the overall rotation. The hyperradial motion corresponds to the symmetric stretching vibration. When the rovibrational wave function is expanded in terms of the harmonics, a system of coupled equations expressed in terms of the hyperradius is obtained. This system is integrated numerically. As the hyperspherical harmonics describe the rotational problem analytically, the size of the expansion does not scale unfavorably with the rotational quantum number J. This is an attractive feature of the harmonics approach. We also note that the harmonics are readily symmetrized [45].

Despite the intrinsic accuracy of the method, a problem arises in relation to the lack of the separability of the vibrational and rotational motions in the Hamiltonian and, thus, only one reduced mass appears. It is the three-particle reduced mass $\mu = \sqrt{m_A m_B m_C/(m_A + m_B + m_C)}$. To deal with this issue the following has been done. First, the calculations of pure vibrational states ($J = 0$) have been performed with the reduced mass obtained from the vibrational nuclear masses, while for the rovibrational calculations of the states with $J \neq 0$ rotational masses have been used. To obtain the desired term values for the case where the vibrational and rotational masses are different, a "fake" $J = 0$ vibrational calculation has been performed using the rotational mass. The rotational-term values obtained in this calculation are then added to the band origins calculated with vibrational masses to yield the final rovibrational energies:

$$\begin{aligned} E(v_1, v_2, J, G; \mu_{\text{vib}}, \mu_{\text{rot}}) = {} & E(v_1, v_2, 0, 0; \mu_{\text{vib}}, \mu_{\text{vib}}) \\ & + \{E(v_1, v_2, J, G; \mu_{\text{rot}}, \mu_{\text{rot}}) \\ & - E(v_1, v_2, 0, 0; \mu_{\text{rot}}, \mu_{\text{rot}})\}. \quad (12) \end{aligned}$$

TABLE I. Numerical values of the dimensionless parameter p, $p = (m_{vib} - m_p)/m_e$ or $p = (m_{rot} - m_p)/m_e$, from which the vibrational and rotational masses, m_{vib} and m_{rot}, may be calculated. The scaled core mass is the core mass multiplied by $f = 0.90$. The empirical rotational mass is calculated using the parametrization given in Eq. (14). It can be improved by scaling the parameter R_T. The numerical value $R_T = 3.026a_0$, which is close of that of the H_2 molecule, yields the optimized values of $p = 0.1118$.

			Vibrational			
			Core mass		Scaled core mass	
Nuclear (both states)	Moss (both states)	NU23 (both states)	$(0,0^0)$	$(0,1^1)$	$(0,0^0)$	$(0,1^1)$
0.0	0.4758	0.6667	0.3155	0.3189	0.2839	0.2870

	Rotational		
	Empirical		Averaged empirical, scaled
Nuclear (both states)	$(0,0^0)$	$(0,1^1)$	(both states)
0.0	0.0618	0.0661	0.1118

III. RESULTS AND DISCUSSION

A. Effective masses and comparison with experiment

In their new experiment Wu *et al*. [11] measured twelve rovibrational transitions between the vibrational ground state $(v_1, v_2^{|\ell|}) = (0,0^0)$ and the first excited state $(0,1^1)$ of H_3^+. These very accurate data provide an excellent opportunity to test the performance of the various effective-mass models. For example, the Moss mass model, which has been used before quite successfully, and our model of coordinate-dependent masses can be put into a stringent test. The tests can also help derive more efficient vibrational and rotational masses which better reproduce the experimental transition energies and allow for generating very accurate predictions for rotational terms not yet measured in the experiment. For the tests to be meaningful a very accurate PES is needed in the rovibrational calculations. Such a PES is the GLH3P PES [3,4]. The accuracy

of the *ab initio* energies in the PES and the accuracy of the analytical fit to this PES are better than 0.1 cm^{-1}. GLH3P is employed in the present work.

In the first step the PT [17] nonadiabatic model is tested. The model uses the constant vibrational mass proposed by Moss [15] for H_2^+ and a constant rotational mass, which is derived in the usual way from the nuclear masses (see Table I). The energies of the rovibrational states obtained with the model are presented in Table II. The results of a standard adiabatic calculation are listed for comparison. When comparing the calculated frequencies with the experimental ones, a linear behavior of the deviation as a function of the rovibrational energy is observed. Following Schiffels *et al*. [46], the deviation can be expressed as the following function of the J rotational quantum number:

$$\text{obs.-calc.} = a_0 + a_1 J(J+1). \tag{13}$$

TABLE II. Comparison with experimental data of Wu *et al*. All transitions are from the vibrational ground state to the lowest degenerate state, i.e., $(0,1^1)_u \leftarrow (0,0^0)_l$. $(J,G)_l$ denotes the rotational quantum numbers of the lower state. P, Q, and R denote spectra branches corresponding to $\Delta J = J_l - J_u = -1, 0, 1$, respectively. The G value is conserved, i.e., $\Delta G = 0$. The results obtained in the following different calculations are shown: AD, standard adiabatic calculation with nuclear vibrational and rotational masses; MM, calculation with Moss vibrational mass and nuclear rotational mass; CRM, calculation with core vibrational mass and empirical rotational mass according to Diniz *et al*. [19]; emp, calculation with Moss vibrational mass and nuclear rotational mass with *a posteriori* empirical vibrational and rotational corrections according to Eq. (13); SCRM, calculation with scaled core vibrational mass and scaled averaged rotational mass. RMS is the root-mean-square value for the method. *spread* is the maximum difference between any two values of the deviation. All data are in wave numbers (cm^{-1}).

$\Delta J(J,G)_l$	Obs.	Obs.-calc. (AD)	Obs.-calc. (MM)	Obs.-calc. (CRM)	Obs.-calc. (emp)	Obs.-calc. (SCRM)
$R(3,3)^u$	2918.02561	0.3871	0.0924	0.0160	−0.0003	0.0035
$R(3,3)^l$	2829.92527	0.3911	0.0964	0.0152	0.0037	−0.0008
$R(2,1)^u$	2826.11683	0.3885	0.0939	0.0142	−0.0042	−0.0007
$R(2,2)^u$	2823.13780	0.3911	0.0971	0.0169	−0.0010	0.0020
$R(2,2)^l$	2762.06965	0.3948	0.1002	0.0167	0.0021	−0.0004
$R(1,1)^u$	2726.22025	0.3970	0.1023	0.0182	−0.0010	0.0011
$R(1,0)$	2725.89816	0.3949	0.1003	0.0162	−0.0030	−0.0009
$R(1,1)^l$	2691.44305	0.3999	0.1053	0.0192	0.0020	0.0008
$Q(2,2)$	2554.66586	0.4084	0.1137	0.0237	−0.0002	0.0020
$Q(1,1)$	2545.42036	0.4089	0.1142	0.0234	0.0003	0.0016
$Q(1,0)$	2529.72464	0.4084	0.1138	0.0222	−0.0002	−0.0002
$Q(2,1)^l$	2518.21154	0.4088	0.1141	0.0223	0.0002	−0.0007
RMS		0.3983	0.1040	0.0190	0.0021	0.0015
Spread		0.0218	0.0218	0.0095	0.0079	0.0044

The two adjustable parameters in (13) are the vibrational offset $a_0 = 0.1139$ cm^{-1}, and the rotational correction $a_1 = -0.002\,646\,8$ cm^{-1}. The numerical value of the a_1 parameter is very close to that found by Schiffels *et al.* [46] ($a_1 = 0.002\,043\,6$ cm^{-1} determined as the average value for all vibrational states up to $10\,000$ cm^{-1}). Following the work by Oka and Morino [47], Morong *et al.* [48] related this parameter to the rotational constants and the diagonal elements of the *g* tensor for the rotational magnetic moment. When the calculated rovibrational energy values are corrected using function (13), the accuracy of the predicted rovibrational frequencies is improved by two orders of magnitude. These data, denoted empirical (emp), are also shown in Table II. The parameter a_1 is also used later in this work to derive a more accurate rotational mass.

Let us now examine the results obtained using the core-mass plus rotational-mass (CRM) model, where our vibrational-mass surface is combined with the empirical, coordinate-dependent rotational mass suggested by Diniz *et al.* [19]. This rotational mass changes from the nuclear mass near the equilibrium geometry to the atomic mass at large separations and it is parametrized as

$$m_{A;\text{rot}}(R) = m_A + a\{1 - [1 + e^{\alpha(R - R_T)}]^{-1}\}. \quad (14)$$

Here *a* is the number of electrons at the particular atomic center (for example, $a = 1$ for H_2, $a = \frac{1}{2}$ for H_2^+, and $a = \frac{2}{3}$ for H_3^+), while α is the smoothness parameter and R_T is the turning point. For H_2, the numerical values of these parameters were fixed at $\alpha = 1.5a_0^{-1}$ and $R_T = 3.0a_0$. For a diatomic molecule *X*, Diniz *et al.* proposed the relation $R_T(X) = R_T(H_2)R_{\text{eq}}(X)/R_{\text{eq}}(H_2)$ and $\alpha(X) = \alpha(H_2)/[R_{\text{eq}}(X)/R_{\text{eq}}(H_2)]$, where R_{eq} is the equilibrium distance of the diatomic and $R_{\text{eq}}(H_2) = 1.4a_0$. Applying this procedure to H_3^+, where the equilibrium bond length is $R_{\text{eq}}(H_3^+) = 1.65a_0$, yields a rotational mass surface, from which constant rotational masses for a particular vibrational state are generated using a similar procedure as used before for the vibrational mass, i.e., by calculating the expectation value of the mass surface with the vibrational wave function of the state considered. DVR3D [42] has been used to compute these averages and their numerical values are given in Table I. The masses are then transformed into the reduced masses for the particular chosen coordinate system in the usual way. A comparison of the results obtained with the Moss mass with the results obtained with the core mass combined with the parametrized rotational mass obtained from the Diniz *et al.* procedure shows that the latter are improved by about one order of magnitude (see the CRM results in Table II). Also the spread of the rotational results is significantly reduced, from 0.022 to 0.009 cm^{-1}.

In their work on H_2 and H_2^+, Diniz *et al.* improved their core-mass (CM) results by applying an empirical scaling to the vibrational mass (let us call such a scaled CM approach a SCM approach). The purpose of the scaling is to correct the shortcoming of the Mulliken population analysis which is known to be dependent on the basis set used in the calculation; a larger and more complete basis set does not always give the best Mulliken atomic charges. The problem is related to the distribution of the electronic charge between the diagonal

TABLE III. Rotational term values of the rovibrational state $(0,0^0)$. *J*, *G*, and *s* denote the rotational quantum numbers. Γ is the permutation-inversion symmetry and *n* is an index counting the states with the same symmetry. E_{MM} is the rovibrational energy relative to the hypothetical $J = 0$ zero-point energy calculated with the Moss vibrational mass and the nuclear rotational mass, E_{emp} is the rovibrational energy obtained with the Moss vibrational mass and the nuclear rotational mass and with empirical vibrational and rotational corrections. E_{SCRM} is the rovibrational energy obtained with the scaled core vibrational mass and the scaled averaged rotational mass. The latter is expected to be the most accurate result presented in this work. Data are given in cm^{-1}.

J	*G*	*s*	Γ	*n*	E_{MM} cm^{-1}	E_{emp} cm^{-1}	E_{SCRM} cm^{-1}
0	0	1	A_1'	0	0.000	0.000	0.000
1	1		E''	0	64.128	64.123	64.124
1	0	1	A_2'	0	86.966	86.961	86.961
2	2		E'	0	169.308	169.293	169.298
2	1		E''	0	237.369	237.353	237.354
3	3	1	A_2''	0	315.364	315.332	315.346
3	2		E'	0	428.042	428.010	428.016
3	1		E''	0	494.792	494.760	494.762
3	0	1	A_2'	0	516.907	516.875	516.876
4	4		E'	0	502.059	502.006	502.029
4	3	−1	A_2''	0	658.748	658.695	658.708
4	2		E'	1	768.510	768.457	768.465
4	1		E''	0	833.620	833.567	833.570
5	5		E''	0	729.043	728.964	729.000
5	4		E'	0	929.014	928.934	928.959
5	3	1	A_2''	0	1080.536	1080.456	1080.472
5	2		E'	1	1187.159	1187.080	1187.089
5	1		E''	1	1250.365	1250.286	1250.291
5	0	1	A_2'	0	1271.324	1271.245	1271.249
6	6	−1	A_2'	0	995.914	995.803	995.855
6	5		E''	0	1238.503	1238.392	1238.430
6	4		E'	0	1430.777	1430.666	1430.693
6	3	−1	A_2''	0	1577.402	1577.291	1577.309
6	2		E'	1	1679.866	1679.755	1679.768
6	1		E''	1	1740.972	1740.861	1740.870
7	7		E''	0	1302.190	1302.042	1302.114
7	6	1	A_2'	0	1586.656	1586.507	1586.562
7	5		E''	1	1818.218	1818.069	1818.111
7	4		E'	0	2002.544	2002.396	2002.428
7	3	1	A_2''	0	2142.194	2142.046	2142.070
7	2		E'	1	2242.088	2241.940	2241.959
7	1		E''	2	2300.956	2300.808	2300.823
7	0	1	A_2'	1	2320.494	2320.346	2320.360
8	8		E'	0	1647.321	1647.130	1647.224
8	7		E''	0	1972.878	1972.688	1972.762
8	6	−1	A_2'	0	2242.292	2242.101	2242.161
8	5		E''	1	2462.981	2462.790	2462.838
8	4		E'	1	2639.256	2639.066	2639.104
8	3	−1	A_2''	0	2775.792	2775.602	2775.633
8	2		E'	2	2868.997	2868.806	2868.833
8	1		E''	2	2925.538	2925.347	2925.371
9	9	1	A_2''	0	2030.688	2030.450	2030.570
9	8		E'	0	2396.509	2396.270	2396.369
9	7		E''	0	2702.193	2701.954	2702.036
9	6	1	A_2'	0	2957.430	2957.192	2957.260

TABLE III. (*Continued.*)

J	G	s	Γ	n	E_{MM} cm^{-1}	E_{emp} cm^{-1}	E_{SCRM} cm^{-1}
9	5		E''	1	3167.475	3167.237	3167.294
9	4		E'	1	3335.707	3335.469	3335.518
9	3	1	A_2''	1	3461.218	3460.980	3461.023
9	2		E'	2	3555.594	3555.356	3555.394
9	1		E''	2	3609.756	3609.518	3609.553
9	0	1	A_2'	1	3627.749	3627.510	3627.545
10	10		E'	0	2451.613	2451.321	2451.470
10	9	−1	A_2''	0	2856.825	2856.534	2856.659
10	8		E'	1	3197.023	3196.732	3196.839
10	7		E''	0	3484.925	3484.634	3484.726
10	6	−1	A_2'	0	3726.731	3726.439	3726.520
10	5		E''	1	3926.355	3926.063	3926.134
10	4		E'	2	4086.623	4086.332	4086.395
10	3	−1	A_2''	1	4215.444	4215.153	4215.209
10	2		E'	3	4296.831	4296.540	4296.593
10	1		E''	2	4348.576	4348.285	4348.335

and off-diagonal elements of the density matrix. The fact that there is a scaling factor, which, when applied to the results, leads to their uniform improvement, indicates that the core-mass approach is, in principle, valid, but perhaps the Mulliken charges are not the best to use to determine the core masses.

If one studies transitions between just two vibrational states, an exact vibrational mass ratio for the two states can be obtained. To this end, an accurate value of the band origin of the $(0,1^1)$ state relative to the hypothetical ground state $(0,0^0)$ with $J = 0$ (this state is forbidden, the true ground state has $J = 1$), is derived from the experimental data with the help of the a_0 parameter, $E_{acc} = E_{MM} + a_0$. The mass surface is then scaled to reproduce this term exactly. As this scaling factor, which is equal to $f = 0.90$, is close to 1, it indicates that the initial data are quite satisfactory. In Table I we present the numerical values of these scaled core masses.

Let us now turn to the optimization of the rotational mass. As we have seen, the use of the empirical rotational mass surface obtained from simple parametrization of Eq. (14) with the values of the two parameters related to those of H$_2$, as suggested in [19], leads to an immediate improvement of the predicted rotational term values over those obtained with the nuclear masses. The spread of the term values is reduced by nearly 60% to just 0.009 cm^{-1}. However, the rotational spread of the empirically corrected, emp, data is even lower and equal to 0.006 cm^{-1}, which suggests that the rotational mass surface can still be improved. The a_1 parameter can be used to achieve this, just as the a_0 parameter was used to scale the vibrational mass. In general, the direct use of an improved rotational mass in the rovibrational calculations is likely to yield more accurate results than an *a posteriori* empirical correction, because the a_1 parameter is derived from the new experimental data which include states with $J \leqslant 4$. It is reasonable to expect that, when this parameter is used to predict the energies of higher J states, these energies are somewhat less accurate than the energies calculated for the $J \leqslant 4$ states. To scale the rotational-mass correction with the help of the a_1 coefficient, we first assume

TABLE IV. Rotational term values of the vibrational state $(0,1^1)$ (see Table III for details). For comparison, the band origin calculated with the nuclear masses is $E = 2521.5946$ cm^{-1}.

J	G	s	Γ	n	E_{MM} cm^{-1}	E_{emp} cm^{-1}	E_{SCRM} cm^{-1}
0	1		E'	0	2521.300	2521.414	2521.414
1	2		E''	1	2548.056	2548.165	2548.169
1	1		E'	0	2609.434	2609.543	2609.543
1	0	1	A_2''	0	2616.577	2616.685	2616.685
2	3	−1	A_2'	0	2614.168	2614.266	2614.276
2	2		E''	1	2723.861	2723.959	2723.962
2	1		E'	1	2755.466	2755.564	2755.567
2	1		E'	2	2790.246	2790.344	2790.343
2	0	−1	A_2''	0	2812.764	2812.862	2812.860
3	4		E''	1	2719.378	2719.460	2719.480
3	3	1	A_2'	1	2876.747	2876.829	2876.839
3	2		E''	2	2931.278	2931.360	2931.368
3	2		E''	3	2992.349	2992.431	2992.434
3	1		E'	1	3002.810	3002.892	3002.896
3	1		E'	2	3063.392	3063.474	3063.472
3	0	1	A_2''	1	3025.868	3025.950	3025.953
4	5		E'	2	2863.836	2863.897	2863.929
4	4		E''	1	3069.234	3069.295	3069.314
4	3	−1	A_2'	0	3145.193	3145.254	3145.272
4	3	−1	A_2'	1	3233.297	3233.358	3233.368
4	2		E''	2	3260.139	3260.200	3260.210
4	2		E''	3	3351.317	3351.378	3351.380
4	1		E'	3	3326.040	3326.101	3326.108
4	1		E'	4	3423.060	3423.121	3423.119
4	0	−1	A_2''	1	3446.990	3447.051	3447.048
5	6	1	A_2''	1	3047.287	3047.322	3047.370
5	5		E'	2	3300.050	3300.084	3300.117
5	4		E''	2	3396.458	3396.492	3396.522
5	4		E''	3	3510.084	3510.118	3510.138
5	3	1	A_2'	1	3553.269	3553.304	3553.324
5	3	1	A_2'	2	3673.910	3673.944	3673.954
5	2		E''	4	3660.284	3660.318	3660.333
5	2		E''	5	3792.990	3793.024	3793.027
5	1		E'	3	3722.576	3722.610	3722.621
5	1		E'	4	3863.374	3863.408	3863.407
5	0	1	A_2''	2	3743.126	3743.160	3743.170
6	7		E'	2	3269.495	3269.498	3269.565
6	6	−1	A_2''	1	3569.388	3569.390	3569.439
6	5		E'	3	3685.032	3685.035	3685.080
6	5		E'	4	3825.373	3825.376	3825.409
6	4		E''	2	3884.080	3884.082	3884.116
6	4		E''	3	4035.742	4035.745	4035.765
6	3	−1	A_2'	1	4029.999	4030.002	4030.027
6	3	−1	A_2'	3	4202.281	4202.284	4202.295
6	2		E''	4	4129.282	4129.285	4129.305
6	2		E''	5	4309.348	4309.351	4309.356
6	1		E'	5	4188.756	4188.759	4188.775
6	1		E'	6	4378.365	4378.368	4378.369
6	0	−1	A_2''	2	4401.068	4401.071	4401.070
7	8		E''	3	3530.159	3530.125	3530.214
7	7		E'	2	3876.977	3876.942	3877.010
7	6	1	A_2''	1	4010.192	4010.158	4010.222
7	6	1	A_2''	2	4177.876	4177.842	4177.891
7	5		E'	3	4249.926	4249.892	4249.942

TABLE IV. (*Continued.*)

J	G	s	Γ	n	E_{MM} cm^{-1}	E_{emp} cm^{-1}	E_{SCRM} cm^{-1}
7	5		E'	4	4431.665	4431.631	4431.665
7	4		E''	4	4420.266	4420.231	4420.278
7	4		E''	6	4636.019	4635.985	4636.007
7	3	1	A_2'	2	4562.803	4562.768	4562.802
7	3	1	A_2'	4	4793.716	4793.682	4793.697
7	2		E''	7	4663.854	4663.819	4663.847
7	2		E''	8	4892.077	4892.043	4892.055
7	1		E'	5	4720.385	4720.350	4720.375
7	1		E'	6	4961.735	4961.700	4961.706
7	0	1	A_2''	3	4739.264	4739.230	4739.254
8	9	−1	A_2'	1	3828.930	3828.853	3828.967
8	8		E''	3	4222.522	4222.445	4222.535
8	7		E'	3	4371.283	4371.207	4371.293
8	7		E'	4	4567.254	4567.177	4567.246
8	6	−1	A_2''	1	4650.922	4650.846	4650.915
8	6	−1	A_2''	2	4862.789	4862.713	4862.765
8	5		E'	6	4874.389	4874.313	4874.371
8	5		E'	7	5107.274	5107.198	5107.236
8	4		E''	4	5028.414	5028.337	5028.390
8	4		E''	7	5304.918	5304.841	5304.869
8	3	−1	A_2'	2	5171.171	5171.094	5171.137
8	3	−1	A_2'	4	5463.172	5463.096	5463.115
8	2		E''	6	5257.318	5257.241	5257.280
8	2		E''	8	5532.844	5532.767	5532.790
8	1		E'	8	5313.008	5312.932	5312.968
8	1		E'	9	5606.850	5606.774	5606.787
8	0	−1	A_2''	3	5629.142	5629.066	5629.078
9	10		E''	3	4165.416	4165.292	4165.434
9	9	1	A_2'	2	4605.675	4605.551	4605.666
9	8		E''	4	4767.560	4767.436	4767.549
9	8		E''	5	4992.962	4992.838	4992.930
9	7		E'	3	5086.325	5086.201	5086.294
9	7		E'	4	5328.337	5328.213	5328.286
9	6	1	A_2''	3	5342.110	5341.986	5342.066
9	6	1	A_2''	4	5610.362	5610.238	5610.296
9	5		E'	6	5565.312	5565.188	5565.259
9	5		E'	7	5842.955	5842.831	5842.877
9	4		E''	6	5689.727	5689.602	5689.668
9	4		E''	9	6031.773	6031.649	6031.685
9	3	1	A_2'	3	5809.441	5809.317	5809.376
9	3	1	A_2'	5	6175.288	6175.163	6175.194
9	2		E''	8	5908.718	5908.594	5908.647
9	2		E''	10	6225.777	6225.652	6225.690
9	1		E'	8	5962.228	5962.103	5962.154
9	1		E'	9	6306.920	6306.796	6306.822
9	0	1	A_2''	5	5979.253	5979.129	5979.179
10	11		E'	4	4539.202	4539.025	4539.199
10	10		E''	3	5026.071	5025.894	5026.037
10	9	−1	A_2'	1	5198.209	5198.031	5198.173
10	9	−1	A_2'	2	5454.437	5454.260	5454.379
10	8		E''	4	5555.443	5555.266	5555.387
10	8		E''	5	5827.756	5827.578	5827.676
10	7		E'	6	5842.751	5842.573	5842.680
10	7		E'	7	6145.304	6145.126	6145.208
10	6	−1	A_2''	3	6087.576	6087.399	6087.493
10	6	−1	A_2''	4	6412.407	6412.230	6412.298
10	5		E'	8	6226.836	6226.658	6226.753

TABLE IV. (*Continued.*)

J	G	s	Γ	n	E_{MM} cm^{-1}	E_{emp} cm^{-1}	E_{SCRM} cm^{-1}
10	5		E'	10	6628.757	6628.580	6628.640
10	4		E''	6	6401.193	6401.016	6401.098
10	4		E''	9	6811.884	6811.706	6811.755
10	3	−1	A_2'	3	6540.009	6539.832	6539.906
10	3	−1	A_2'	6	6959.188	6959.011	6959.053
10	2		E''	8	6612.545	6612.368	6612.439
10	2		E''	10	6967.507	6967.330	6967.385
10	1		E'	11	6666.175	6665.998	6666.065
10	1		E'	13	7055.466	7055.288	7055.332
10	0	−1	A_2''	5	7080.594	7080.416	7080.457

the following expansion for the energy of the J rotational state:

$$E_{\text{rot}}(J) = BJ(J+1) + (C-B)G^2 + \cdots, \quad (15)$$

which includes the lowest order term in $J(J+1)$ and a G term for nondegenerate vibrational states, i.e., $l = 0$. B and C are rotational constants. At equilibrium $B \approx 2C$. A higher order expression of the rotational energy was given by Watson [49], but is not needed here. The rotational constant B is inversely proportional to the rotational reduced mass, which itself is proportional to the effective atomic mass. In hyperspherical coordinates, for example, it is equal to the three-particle reduced mass, $\mu_{\text{rot}} = m_{\text{nuc}}/\sqrt{3}$. Hence we obtain

$$\frac{B + a_1}{B} = \frac{m_{\text{nuc}}}{m_{\text{rot}}}. \quad (16)$$

The rotational mass m_{rot} is readily obtained from this equation. The value of B is computed from the $J = 0$ and $J = 1$ states with $G = 0$ corresponding to the vibrational ground state ($v_1 = 0$, $v_2 = 0$, $l = 0$) using Eq. (15):

$$B = \frac{E(J=1, G=0) - E(J=0, G=0)}{2}. \quad (17)$$

These states were chosen since $\Delta G = 0$ and hence the second term in Eq. (15) vanishes. The numerical value of the rotational constant and thus the rotational mass derived from it is much more accurate than the simple formula may suggest. This rotational mass can be used to scale the turning point parameter R_T of the empirical formula, Eq. (14). We employ such scaling in the rovibrational calculations involving the two lowest vibrational states (see Table I). The use of the same rotational mass for the two vibrational states is justified by the fact that the a_1 parameter corrects rotational transition energies rather than the individual term values. Furthermore, the numerical value of this parameter was determined from a calculation with identical rotational masses.

When a full rovibrational calculation is performed with these masses and the scaled core masses are used as vibrational masses, very accurate results are obtained. This model involving the scaled core vibrational masses and the scaled averaged rotational masses is denoted as SCRM in the further discussion. The SCRM results and their comparison with the experimental results and with the results obtained with the other models are presented in Table II. For higher values of J the SCRM predictions are expected to be more accurate than the empirical
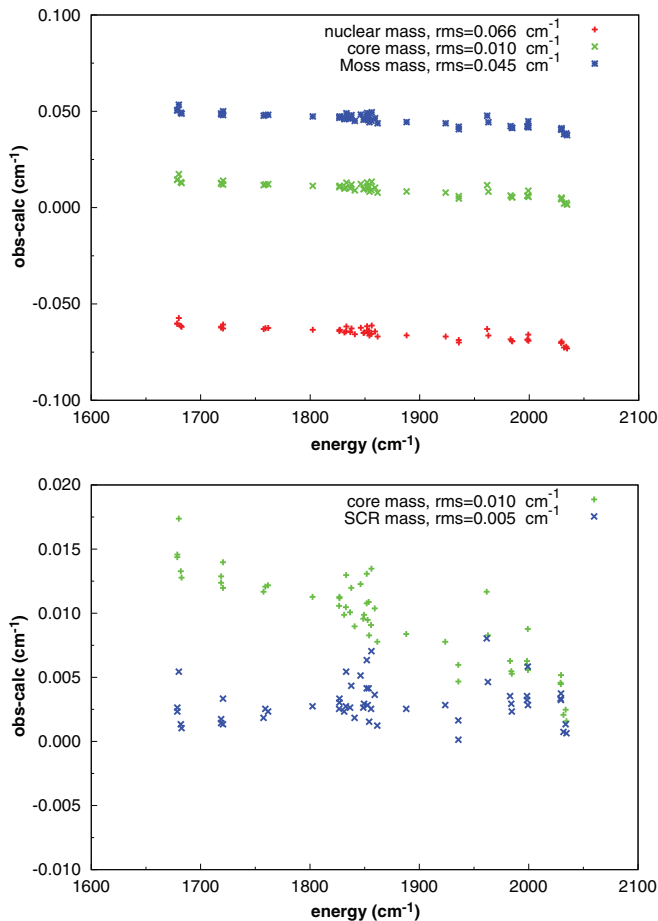
FIG. 2. (Color online) Comparison of experimental D_3^+ transition frequencies with calculated values obtained using different effective nuclear masses.

(emp) ones. A selective check with the experimentally derived term values by Lindsay and McCall [10] confirms this.

We have also performed a test to verify if the mass-surface approach works equally well for D_3^+ as it does for H_3^+. The $(0,1^1)$ fundamental band of D_3^+ has been studied experimentally [50–52]. Of the measured frequencies, we have analyzed those for transitions with $J \leqslant 4$, i.e., 54 transitions. Figure 2 gives a comparison of the predictions for these 54 transitions with different treatments of the effective mass. As can be seen, use of the nuclear mass ($m_d = 2.013\,532\,13$ u) or Moss mass ($m_D = 2.013\,814\,0$ u) give significantly worse results than use of the core mass [$m_D = m_d + 0.3138m_e = 2.013\,725\,34$ u for $(0,0^0)$ and $m_D = m_d + 0.3162m_e = 2.013\,726\,66$ u for $(0,1^1)$]. Furthermore, use of the SCRM, with a scaling factor of the vibrational mass of 0.9, as used for H_3^+, and a rotational mass of $m_d + 0.1118m_e$, same increment as for H_3^+, give a further factor of 2 improvement in our predictions. The residual is only 0.0025 cm^{-1}, which may be compared with the experimental error bar of 0.002 cm^{-1} [51,52] and 0.0005 cm^{-1} [50].

B. Calculated rotational term values for the two lowest vibrational states

The SCRM model is used together with the GLH3P potential energy surface to compute very accurate term values for the

two lowest vibrational states. The calculations are performed with the hyperspherical code assuming full symmetry. The absolute error of the SCRM term values is of the order of 0.01 cm^{-1}, while the frequencies derived from these term values are expected to be even more accurate. Hence our theoretical predictions are approaching the accuracy of the previous experiments.

The spectroscopic assignments provided by Schiffels *et al*. [53] for the $J \leqslant 7$ state are used. States with higher J are assigned on the basis of their symmetry using the procedure described by Schiffels *et al*. Some of them can be compared with the list of states derived from the experimental data by Lindsay and McCall [10]. For higher values of J, some assignments become ambiguous due to strong level mixing. For this reason, we limit the calculation in this work to states with $J \leqslant 10$. No experimentally derived term values are available for the rovibrational states $(0,0^0)$ with $J = 10$, $G = 10$ and $J = 10$, $G = 2$ and $(0,1^1)$ with $J = 10$, $G = 11$, $J = 10$, $G = 10$, and $J = 10$, $G = 2$.

IV. CONCLUSIONS

When a molecule vibrates, the atoms forming the system move about their equilibrium positions. This motion involves the nuclei of the atoms and some part of the electrons. It is reasonable to assume that all inner-shell (core) electrons move along with the vibrating nuclei, but only a part of the valence electrons is involved in this motion. It is also reasonable to assume that the electron density, which closely follows the nuclei in the vibrational motion, is not constant but depends on the geometry of the molecule in the particular phase of the motion. For example, for a diatomic molecule connected with a covalent bond the number of electrons which moves along with the nuclei when the geometry of the molecule is near the equilibrium geometry can be expected to be smaller than the number of the moving electrons at a geometry where the bond is elongated. This is because some of the electrons at equilibrium are involved in the bonding and do not move with the nuclei, while, when the bond is almost broken, some of the bonding electrons join the core electrons in following the nuclei in their vibrational motion. This simple picture suggests that one can easily improve the accuracy of the calculation of the rovibrational states of a molecule by adding some electronic mass to each nuclear mass and using such effective vibrational masses in the vibrational calculations. Furthermore, one can make these effective masses dependent on the molecular geometry.

The effective vibrational-mass model of Mohallem and co-workers (i.e., the core-mass model) is considered in this work in the calculation of the rovibrational spectrum of the H_3^+ ion. The effective masses are obtained from the diagonal terms resulting from the Mulliken population analysis. It is shown that the model gives much improved results in comparison to using nuclear masses as the vibrational masses. It also gives improved results in comparison with the model of Bunker and Moss where the masses are determined from the analysis of the nonadiabatic corrections to the nuclear wave functions obtained from perturbation-theory calculations. Further improvement of the results is obtained by applying empirical scaling to the effective masses. The effective-mass model

developed in this work is used to predict energies of some rovibrational states of H_3^+, which have not been measured yet. The predictions concern transition frequencies for highly excited rotational states and the two lowest vibrational states.

This work also shows that by using a simple, physically motivated, effective-mass model based on the Mulliken population analysis one can bypass the computational bottleneck of evaluating nonadiabatic corrections to the rovibrational levels with the use of the perturbation theory. Despite the simplicity of the effective-mass model very accurate results are obtained. Whether the model is equally accurate in describing states where both vibrational and rotational motions are excited to higher levels requires more testing. Such tests should be performed for the highest states known from the experiment near 16 000 cm^{-1}. There are also some theoretical issues in variable-mass calculations which need to be addressed. For example, Pachucki and Komasa [54] showed that the effective masses computed for H_2 using rigorous nonadiabatic theory can be larger than the masses of the nuclei plus the electron masses for internuclear distances near 4 a.u. However, these internuclear distances are only accessed in H_2 in highly excited vibrational states. Another issue is the problem with imposing the correct permutational symmetry in the rovibrational wave function. Using different geometry-dependent vibrational masses for the three H_3^+ nuclei makes them "distinguishable." A question which arises is, can one still symmetry adapt the nuclear wave function? There is also a related question concerning the form of the kinetic energy operator representing the rovibrational motion. These issues will be discussed in our future work as will the treatment of asymmetric isotopologues whose spectra are known to be particularly sensitive to beyond Born-Oppenheimer effects [55].

[1] T. R. Geballe and T. Oka, Science **312**, 1610 (2006).

[2] A. Alijah, J. Mol. Spectrosc. **264**, 111 (2010).

[3] M. Pavanello, L. Adamowicz, A. Alijah, N. F. Zobov, I. I. Mizus, O. L. Polyansky, J. Tennyson, T. Szidarovszky, A. G. Császár, M. Berg, A. Petrignani, and A. Wolf, Phys. Rev. Lett. **108**, 023002 (2012).

[4] M. Pavanello, L. Adamowicz, A. Alijah, N. F. Zobov, I. I. Mizus, O. L. Polyansky, J. Tennyson, T. Szidarovszky, and A. G. Császár, J. Chem. Phys. **136**, 184303 (2012).

[5] L. Adamowicz and M. Pavanello, Philos. Trans. R. Soc. London, Ser. A **370**, 5001 (2012).

[6] O. L. Polyansky, A. Alijah, N. F. Zobov, I. I. Mizus, R. I. Ovsyannikov, J. Tennyson, L. Lodi, T. Szidarovszky, and A. G. Császár, Philos. Trans. R. Soc. London, Ser. A **370**, 5014 (2012).

[7] R. Jaquet and M. V. Khoma, J. Chem. Phys. **136**, 154307 (2012).

[8] R. Jaquet and T. Carrington, J. Phys. Chem. A (to be published).

[9] R. A. Bachorz, W. Cencek, R. Jaquet, and J. Komasa, J. Chem. Phys. **131**, 024105 (2009).

[10] C. M. Lindsay and B. J. McCall, J. Mol. Spectrosc. **210**, 60 (2001).

[11] K.-Y. Wu, Y.-H. Lien, C.-C. Liao, Y.-R. Lin, and J.-T. Shy, following paper, Phys. Rev. A **88**, 032507 (2013).

[12] J. A. Coxon and P. G. Hajigeorgiou, J. Mol. Spectrosc. **193**, 306 (1999).

[13] P. R. Bunker and R. E. Moss, Mol. Phys. **33**, 417 (1977).

[14] P. R. Bunker and R. E. Moss, J. Mol. Spectrosc. **80**, 217 (1980).

[15] R. E. Moss, Mol. Phys. **89**, 195 (1996).

[16] R. Jaquet and W. Kutzelnigg, Chem. Phys. **346**, 69 (2008).

[17] O. L. Polyansky and J. Tennyson, J. Chem. Phys. **110**, 5056 (1999).

[18] J. R. Mohallem, L. G. Diniz, and A. S. Dutra, Chem. Phys. Lett. **501**, 575 (2011).

[19] L. G. Diniz, A. Alijah, and J. R. Mohallem, J. Chem. Phys. **137**, 164316 (2012).

[20] R. E. Moss and D. Jopling, Chem. Phys. Lett. **260**, 377 (1996).

[21] P. R. Bunker, C. J. McLarnon, and R. E. Moss, Mol. Phys. **33**, 425 (1977).

[22] B. M. Dinelli, L. Neale, O. L. Polyansky, and J. Tennyson, J. Mol. Spectrosc. **163**, 71 (1994).

[23] J. K. G. Watson, Chem. Phys. **190**, 291 (1995).

[24] R. Jaquet, W. Cencek, W. Kutzelnigg, and J. Rychlewski, J. Chem. Phys. **108**, 2837 (1998).

[25] R. Jaquet, in *Explicitly Correlated Wave Functions in Chemistry and Physics*, Progress in Theoretical Chemistry and Physics, edited by J. Rychlewski (Kluwer Academic Publishers, Dordrecht, The Netherlands, 2003), Vol. 13.

[26] D. W. Schwenke, J. Chem. Phys. **114**, 1693 (2001).

[27] D. W. Schwenke, J. Phys. Chem. A **105**, 2352 (2001).

[28] R. Jaquet and M. V. Khoma, Mol. Phys. **110**, 669 (2012).

[29] R. Jaquet and M. V. Khoma, Mol. Phys. **110**, 3105 (2012).

[30] R. M. Herman and A. Asgharian, J. Mol. Spectrosc. **19**, 305 (1966).

[31] R. S. Mulliken, J. Chem. Phys. **23**, 1833 (1955).

[32] J. J. Munro, J. Ramanlal, and J. Tennyson, New J. Phys. **7**, 196 (2005).

[33] J. N. Murrell, S. Carter, S. C. Farantos, P. Huxley, and A. J. C. Varandas, *Molecular Potential Energy Functions* (Wiley, Chichester, 1984).

[34] L. Neale, S. Miller, and J. Tennyson, Astrophys. J. **464**, 516 (1995).

[35] A. J. C. Varandas, Adv. Chem. Phys. **74**, 255 (1988).

[36] M. W. Schmidt, K. K. Baldridge, J. A. Boats, S. T. Elbert, M. S. Gordon, J. H. Jensen, S. Koseki, N. Matsunaga, K. A. Nguyen, S. Su, T. Windus, M. Dupuis, and J. Montgomery, J. Comput. Chem. **14**, 1347 (1993).

[37] M. S. Gordon and M. W. Schmidt, in *Theory and Applications of Computational Chemistry: The First Forty Years*, edited by C. E. Dykstra, G. Frenking, K. S. Kim, and G. E. Scuseria (Elsevier, Amsterdam, 2005), pp. 1167–1189.

[38] W. Meyer, P. Botschwina, and P. R. Burton, J. Chem. Phys. **84**, 891 (1986).

[39] O. L. Polyansky, R. Prosmiti, W. Klopper, and J. Tennyson, Mol. Phys. **98**, 261 (2000).

[40] L. P. Viegas, A. Alijah, and A. J. C. Varandas, J. Chem. Phys. **126**, 074309 (2007).

[41] H. Weyl, *The Classical Theory of Groups* (Princeton University Press, Princeton, NJ, 1946).

[42] J. Tennyson, J. R. Henderson, and N. G. Fulton, Comput. Phys. Commun. **86**, 175 (1995).

[43] L. Wolniewicz, J. Chem. Phys. **90**, 371 (1989).

[44] B. R. Johnson, J. Chem. Phys. **73**, 5051 (1980).

[45] L. Wolniewicz, J. Hinze, and A. Alijah, J. Chem. Phys. **99**, 2695 (1993).

[46] P. Schiffels, A. Alijah, and J. Hinze, Mol. Phys. **101**, 175 (2003).

[47] T. Oka and Y. Morino, J. Mol. Spectrosc. **6**, 472 (1961).

[48] C. P. Morong, J. L. Gottfried, and T. Oka, J. Mol. Spectrosc. **255**, 13 (2009).

[49] J. K. G. Watson, J. Mol. Spectrosc. **103**, 350 (1984).

[50] J.-T. Shy, J. W. Farley, W. E. Lamb, Jr., and W. H. Wing, Phys. Rev. Lett. **45**, 535 (1980).

[51] J. K. G. Watson, S. C. Foster, and A. R. W. McKellar, Can. J. Phys. **65**, 38 (1986).

[52] T. Amano, M.-C. Chan, S. Civiš, A. R. W. McKellar, W. A. Majewski, D. Sadovskií, and J. K. G. Watson, Can. J. Phys. **72**, 1007 (1994).

[53] P. Schiffels, A. Alijah, and J. Hinze, Mol. Phys. **101**, 189 (2003).

[54] K. Pachucki and J. Komasa, J. Chem. Phys. **130**, 164113 (2009).

[55] B. M. Dinelli, C. R. LeSueur, J. Tennyson, and R. D. Amos, Chem. Phys. Lett. **232**, 295 (1995).